

# A Novel Scheme for Joint Estimation of Velocity, Angle-of-arrival and Range in Multipath Environment

Zhiyu Yang, Rui Wang and Yi Jiang

School of Information Science and Technology, Fudan University, Shanghai, China  
Email: yangzy19@fudan.edu.cn, ruiwang18@fudan.edu.cn, yjiang@fudan.edu.cn

**Abstract**—The estimation of velocity, angle-of-arrival (AOA), and range of a target has been researched for decades, as it finds wide applications in radar and wireless communications. In recent years, this classic problem has gained renewed interest with the advent of 5G internet of things (IoT) technologies, owing to the numerous emerging localization-related applications. This paper studies the joint estimation of velocity, AOA, and range (JEVAR) of a target in a multipath environment. To solve the JEVAR problem, we propose a novel scheme, which has the target transmit a pair of conjugate Zadoff-Chu (ZC) sequences and has the multi-antenna receiver conduct maximum likelihood (ML) estimation. The simulations verify the effectiveness of the proposed scheme by showing that its performance can approach the Cramer-Rao bound (CRB).

**Index Terms**—angle-of-arrival, velocity, range, Zadoff-Chu sequences, maximum likelihood estimation, Cramer-Rao bound

## I. INTRODUCTION

The estimation of velocity (via estimating Doppler frequency offset), angle-of-arrival (AOA), and range (via estimating time delay) of a target, is a classic radar signal processing problem. In recent years, this problem has gained great interest outside of the radar community, owing to the numerous localization-related applications emerging with the advent of 5G internet of things (IoT) technologies, including indoor localization [1] and autonomous driving [2].

The joint estimation of velocity, AOA, and range, which we term as the JEVAR problem, was originally proposed for wireless channel estimation in [3] and was later studied for the global navigation satellite systems (GNSS) in [4]. The JEVAR problem also arises from various IoT applications, such as autonomous driving and indoor localization/navigation, as the estimates of the velocities, angles, and ranges of a source in the multipath environment can be combined for high-precision localization. In a dense urban or indoor environment, however, the JEVAR problem is challenging due to the multipath interferences.

In [3] [4], the space-alternating generalized expectation-maximization (SAGE) method is utilized to transform the high-dimensional parameter optimization problem to multiple lower-dimensional ones. But even for the single-path line-of-sight (LOS) case, the JEVAR is a challenging three-dimensional searching problem, especially when the uncer-

tainty ranges of the time delay and frequency offset are large.

In this paper, we consider the JEVAR problem in the multipath environment. By borrowing the idea of using conjugate Zadoff-Chu (ZC) sequences [5], we propose a novel and more efficient solution, which has the target transmit a pair of conjugate ZC sequences and has the multi-antenna receiver conduct maximum likelihood (ML) estimation. By exploiting the ZC sequences' time delay-frequency offset ambiguity, the estimate of time delay and frequency offset can be obtained in a reduced dimension. The numerical simulation shows that the root mean square error (RMSE) performance of the proposed scheme can approach the CRB. Moreover, the proposed scheme can significantly outperform the state-of-the-art methods in differentiating closely-spaced multipaths. Even with only 20 MHz bandwidth (it is WiFi's bandwidth on the 2.4GHz frequency band), the proposed scheme can achieve range estimation precision of centimeter-level, AOA estimation precision of  $0.01^\circ$ , and velocity estimation precision of one meter per second (m/s), which makes the proposed scheme a promising technology for the localization and navigation related IoT applications.

## II. SIGNAL MODEL AND PROBLEM FORMULATION

### A. Signal Model

Consider an  $M$ -element uniform linear array (ULA) at the receiver. The steering vector  $\mathbf{a}(\theta)$  with respect to the AOA  $\theta$  can be written as

$$\mathbf{a}(\theta) = [1, e^{-j\frac{2\pi d}{\lambda} \sin \theta}, e^{-j\frac{4\pi d}{\lambda} \sin \theta}, \dots, e^{-j\frac{2\pi d(M-1)}{\lambda} \sin \theta}]^T, \quad (1)$$

where  $d$  is the inter-antenna spacing and  $\lambda$  is the carrier wavelength.

In a multipath environment, the continuous time signal received by the antenna array consists of a LOS path and  $U-1$  reflections of a known pilot signal  $x(t)$ , superimposed by the additive white Gaussian noise  $\mathbf{z}(t)$ , i.e.,

$$\mathbf{y}(t) = \sum_{u=1}^U \beta_u \mathbf{a}(\theta_u) x(t - \tau_u) e^{j2\pi \xi_u t} + \mathbf{z}(t), t \in \mathbb{R}, \quad (2)$$

where  $\theta_u$ ,  $\tau_u$ ,  $\xi_u$ , and  $\beta_u$  denote the AOA, time delay, Doppler frequency offset, and the complex channel gain of the  $u$ th path, respectively.

The sampled signal  $y(nT_s)$  after the receiver's analog-to-digital converters (ADC) consists of  $L$  snapshots with  $n = 0, 1, \dots, L-1$ , where  $T_s$  is the Nyquist sampling

Work in this paper was supported by the National Natural Science Foundation of China grant No. 61771005.

interval. For notational simplicity, we denote  $T_s = 1$ , and thus obtain the discrete time signal

$$\mathbf{y}(n) = \sum_{u=1}^U \beta_u \mathbf{a}(\theta_u) x(n - \tau_u) e^{j2\pi\xi_u n} + \mathbf{z}(n), \quad (3)$$

where  $\tau_u \in \mathbb{R}$  is not necessarily an integer.

We assume that  $L$  samples, with indices from  $-L/2$  to  $L/2 - 1$ , are processed [if  $L$  is an odd number, the indices are from  $-(L-1)/2$  to  $(L-1)/2$ ]. The index range differs from the convention to cater to the proposed special design of the pilot  $x(t)$ , as we will see soon in Section III.

By formatting

$$\boldsymbol{\tau} = [\tau_1, \tau_2, \dots, \tau_U]^T \in \mathbb{R}^U,$$

$$\boldsymbol{\xi} = [\xi_1, \xi_2, \dots, \xi_U]^T \in \mathbb{R}^U,$$

$$\boldsymbol{\theta} = [\theta_1, \theta_2, \dots, \theta_U]^T \in \mathbb{R}^U,$$

$$\boldsymbol{\beta} = [\beta_1, \beta_2, \dots, \beta_U]^T \in \mathbb{C}^U,$$

$$\mathbf{A}(\boldsymbol{\theta}) = [\mathbf{a}(\theta_1), \mathbf{a}(\theta_2), \dots, \mathbf{a}(\theta_U)] \in \mathbb{C}^{M \times U},$$

$$\mathbf{Y} = [\mathbf{y}(-\frac{L}{2}), \mathbf{y}(-\frac{L}{2} + 1), \dots, \mathbf{y}(\frac{L}{2} - 1)] \in \mathbb{C}^{M \times L},$$

and

$$\mathbf{Z} = \left[ \mathbf{z}(-\frac{L}{2}), \mathbf{z}(-\frac{L}{2} + 1), \dots, \mathbf{z}(\frac{L}{2} - 1) \right] \in \mathbb{C}^{M \times L}, \quad (4)$$

we reformulate (3) as

$$\mathbf{Y} = \mathbf{A}(\boldsymbol{\theta}) \text{diag}(\boldsymbol{\beta}) \mathbf{X}(\boldsymbol{\tau}, \boldsymbol{\xi})^T + \mathbf{Z}, \quad (5)$$

where

$$\mathbf{X}(\boldsymbol{\tau}, \boldsymbol{\xi}) = [\mathbf{x}(\tau_1) \odot \mathbf{d}(\xi_1), \dots, \mathbf{x}(\tau_U) \odot \mathbf{d}(\xi_U)] \in \mathbb{C}^{L \times U}, \quad (6)$$

with

$$\mathbf{x}(\tau_u) = \begin{bmatrix} x(-\frac{L}{2} - \tau_u) \\ x(-\frac{L}{2} + 1 - \tau_u) \\ \dots \\ x(\frac{L}{2} - 1 - \tau_u) \end{bmatrix}, \quad \mathbf{d}(\xi_u) = \begin{bmatrix} e^{j2\pi\xi_u(-\frac{L}{2})} \\ e^{j2\pi\xi_u(-\frac{L}{2}+1)} \\ \vdots \\ e^{j2\pi\xi_u(\frac{L}{2}-1)} \end{bmatrix}. \quad (7)$$

### B. Problem Formulation

Because the elements of  $\mathbf{Z}$  are of i.i.d. white Gaussian distribution, the ML estimation of the parameters  $\{\boldsymbol{\beta}, \boldsymbol{\tau}, \boldsymbol{\xi}, \boldsymbol{\theta}\}$  can be readily derived into the least square form:

$$\{\hat{\boldsymbol{\beta}}, \hat{\boldsymbol{\tau}}, \hat{\boldsymbol{\xi}}, \hat{\boldsymbol{\theta}}\} = \arg \min_{\boldsymbol{\beta}, \boldsymbol{\tau}, \boldsymbol{\xi}, \boldsymbol{\theta}} \left\| \mathbf{Y} - \mathbf{A}(\boldsymbol{\theta}) \text{diag}(\boldsymbol{\beta}) \mathbf{X}(\boldsymbol{\tau}, \boldsymbol{\xi})^T \right\|_F^2. \quad (8)$$

Since  $\text{vec}(\mathbf{ABC}^T) = (\mathbf{C} \otimes \mathbf{A}) \text{vec}(\mathbf{B})$ , we have

$$\text{vec}(\mathbf{A}(\boldsymbol{\theta}) \text{diag}(\boldsymbol{\beta}) \mathbf{X}(\boldsymbol{\tau}, \boldsymbol{\xi})^T) = \tilde{\mathbf{X}} \boldsymbol{\beta}, \quad (9)$$

where

$$\tilde{\mathbf{X}} = [\tilde{\mathbf{x}}_1, \tilde{\mathbf{x}}_2, \dots, \tilde{\mathbf{x}}_U] \in \mathbb{C}^{LM \times U}, \quad (10)$$

$$\tilde{\mathbf{x}}_u = [\mathbf{x}(\tau_u) \odot \mathbf{d}(\xi_u)] \otimes \mathbf{a}(\theta_u) \in \mathbb{C}^{LM \times 1}, u = 1, \dots, U. \quad (11)$$

Thus, (8) can be rewritten as

$$\{\hat{\boldsymbol{\beta}}, \hat{\boldsymbol{\tau}}, \hat{\boldsymbol{\xi}}, \hat{\boldsymbol{\theta}}\} = \arg \min_{\boldsymbol{\beta}, \boldsymbol{\tau}, \boldsymbol{\xi}, \boldsymbol{\theta}} \left\| \text{vec}(\mathbf{Y}) - \tilde{\mathbf{X}} \boldsymbol{\beta} \right\|^2. \quad (12)$$

Denote  $\tilde{\mathbf{y}} \triangleq \text{vec}(\mathbf{Y})$ , the ML estimate of  $\boldsymbol{\beta}$  is

$$\hat{\boldsymbol{\beta}} = (\tilde{\mathbf{X}}^H \tilde{\mathbf{X}})^{-1} \tilde{\mathbf{X}}^H \tilde{\mathbf{y}}. \quad (13)$$

Inserting (13) into (12) yields

$$\{\hat{\boldsymbol{\tau}}, \hat{\boldsymbol{\xi}}, \hat{\boldsymbol{\theta}}\} = \arg \max_{\boldsymbol{\tau}, \boldsymbol{\xi}, \boldsymbol{\theta}} \tilde{\mathbf{y}}^H \mathcal{P}(\tilde{\mathbf{X}}) \tilde{\mathbf{y}}, \quad (14)$$

where  $\mathcal{P}(\tilde{\mathbf{X}}) \triangleq \tilde{\mathbf{X}}(\tilde{\mathbf{X}}^H \tilde{\mathbf{X}})^{-1} \tilde{\mathbf{X}}^H$  is the projection matrix of  $\tilde{\mathbf{X}}$ .

The JEVAR problem (14) is the focus of this paper, which appears difficult as it involves non-convex optimization in a  $3U$ -dimensional space. To obtain an efficient solution, we i) use a conjugate pair of Zadoff-Chu sequences as the pilot to decouple the estimation of the time delays and frequency offsets, and ii) use an alternating projection (AP) method [6] on the receiver side to obtain the optimum solution.

We first elaborate the design of the pilot and illustrate its benefit in Section III.

## III. THE PILOT DESIGN BASED ON CONJUGATE ZC SEQUENCES

### A. Properties of ZC Sequence

A length- $\tilde{L}$  ZC sequence is [7]

$$s(n) = \begin{cases} e^{\frac{j\pi r n(n+1)}{\tilde{L}}} & \text{if } \tilde{L} \text{ is odd} \\ e^{\frac{j\pi r n^2}{\tilde{L}}} & \text{if } \tilde{L} \text{ is even} \end{cases}, \quad (15)$$

where the index  $r$  is a positive integer co-prime to  $\tilde{L}$ .

It is easy to verify that  $s(n) = s(n + \tilde{L})$ , i.e., the ZC is periodic. Hence we can set the index range of the ZC to be from  $-\tilde{L}/2$  to  $\tilde{L}/2 - 1$  for an even  $\tilde{L}$ , or from  $-(\tilde{L}-1)/2$  to  $(\tilde{L}-1)/2$  for an odd  $\tilde{L}$ .

For an even  $\tilde{L}$  and an integer delay  $\tau$ , we have

$$s(n - \tau) = e^{\frac{j\pi r(n-\tau)^2}{\tilde{L}}} = e^{\frac{j\pi r \tau^2}{\tilde{L}}} e^{-\frac{j2\pi r \tau n}{\tilde{L}}} s(n). \quad (16)$$

That is, an integer delay  $\tau$  amounts to a frequency offset  $-r\tau/\tilde{L}$ ; the same property also holds for an odd-length ZC. This property indicates that the time delay and frequency offset cannot be uniquely determined based on a single ZC sequence. In paper [5], the authors propose to resolve this ambiguity by using a pair of conjugate ZC sequences.

### B. Pulse Shaping of Raised Cosine Filter

The time-frequency ambiguity revealed in (16) only applies to an integer  $\tau$ . But to achieve super-resolution time delay estimation, we need to take into account the pulse shaping filters.

In the JEVAR scheme, we model the pulse shaper as the raised cosine filter with impulse response

$$p(t) = \text{sinc}(t) \frac{\cos(\pi\alpha t)}{1 - (2\alpha t)^2}, \quad (17)$$

where  $\alpha$  is the roll-off factor. With this filtering, the ZC sequence  $s(n)$  becomes a continuous time waveform

$$x(t) = \sum_n s(n) p(t - n), \quad t \in \mathbb{R}. \quad (18)$$

For a chirp signal  $\{s(t) = e^{j\pi t^2/\tilde{L}}, -\tilde{L}/2 \leq t < \tilde{L}/2\}$ , the instantaneous frequency is  $t/\tilde{L}$ . We consider the instantaneous frequency of  $s(t)$  within  $-(1-\alpha)/2 <$

$t/\tilde{L} < (1 - \alpha)/2$  as the low frequency part. Consider a continuous time signal  $x(t)$  which is obtained according to (18): the sequence  $s(n)$  has high frequency and thus will be suppressed by the filter; the mid-part of the sequence has low frequency and thus will be intact. Indeed, the mid-part of the continuous time waveform  $x(t)$  can be approximated as a chirp signal, i.e.,

$$x(t) \approx e^{j\pi t^2/\tilde{L}}, \quad -\frac{L}{2} \leq t < \frac{L}{2}, \quad (19)$$

where  $L < \tilde{L}$  and we only consider the ZCs with index  $r = 1$  throughout this paper. Fig.1 shows a zoomed-in view of the difference  $|x(t) - e^{j\pi t^2/\tilde{L}}|$  with  $\alpha = 0.3$ ,  $\tilde{L} = 400$ . In this case, the approximation (19) is quite precise for  $L = 250$ .

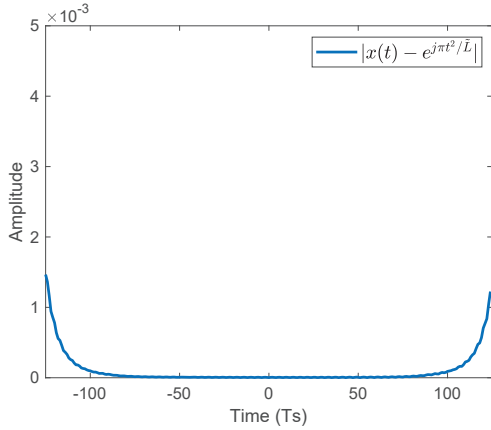


Fig. 1: The approximation (19) is good since  $|x(t) - s(t)| < 1.8 \times 10^{-3}$  for  $-125 \leq t < 125$ .

Now we have established that the lower-frequency part of the ZC sequence pulse shaped by a raised cosine filter can be approximated as a chirp  $x(t) = e^{j\pi t^2/\tilde{L}}$ , which also has the ambiguity between time-delay and frequency-offset:

$$x(t - \tau) = e^{j\frac{\pi\tau^2}{L}} e^{-j\frac{2\pi\tau t}{L}} x(t), \quad (20)$$

where the delay  $\tau$  can be a real-valued number rather than an integer in (16).

Denoting

$$\mathbf{x}(\tau) \triangleq \begin{bmatrix} x(-\frac{L}{2} - \tau) \\ x(-\frac{L}{2} + 1 - \tau) \\ \vdots \\ x(\frac{L}{2} - 1 - \tau) \end{bmatrix}, \mathbf{s} \triangleq \begin{bmatrix} s(-\frac{L}{2}) \\ s(-\frac{L}{2} + 1) \\ \vdots \\ s(\frac{L}{2} - 1) \end{bmatrix}, \quad (21)$$

and recognizing that  $\mathbf{x}(0) = \mathbf{s}$ , we can rewrite (20) in the vector form as

$$\mathbf{x}(\tau) = e^{j\frac{\pi\tau^2}{L}} \mathbf{s} \odot \mathbf{d}\left(-\frac{\tau}{\tilde{L}}\right). \quad (22)$$

### C. The Pilot Design

Inspired by [5], here we also adopt the conjugate pair of ZC sequences as the pilot. But in this paper, we take the pulse shaper filtering into account and recognize that the mid-part of the continuous time waveform  $x(t) = \sum_n s(n)p(t - n)$  can be approximated as a chirp signal.

This observation greatly simplifies the super-resolution estimation of the time delay.

The first half pilot is

$$s(n) = e^{j\pi n^2/\tilde{L}}, n = -\frac{L}{2}, -\frac{L}{2} + 1, \dots, \frac{L}{2} - 1, \quad (23)$$

and the second half is the conjugate of the first half pilot.

For the first half pilot, we propose to append a length- $\frac{Q}{2}$  prefix and a length- $\frac{Q}{2}$  suffix as the protection interval, which can be expressed as

$$prefix = e^{j\pi n^2/\tilde{L}}, n = -\frac{L+Q}{2}, \dots, -\frac{L}{2} - 1, \quad (24)$$

and

$$suffix = e^{j\pi n^2/\tilde{L}}, n = \frac{L}{2}, \dots, \frac{L+Q}{2} - 1. \quad (25)$$

Similarly, the second half pilot has the conjugate prefix and the conjugate suffix. Fig. 2 depicts the structure of the conjugate ZC pilot.

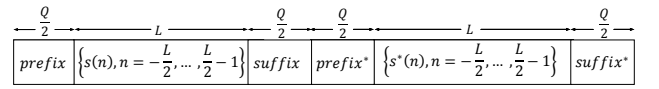


Fig. 2: The pilot sequence structure based on conjugate ZC sequences pair.

## IV. THE JEVAR IN SINGLE-PATH CASE

Before dealing with the JEVAR problem in the multipath scenario in Section V, this section considers the single-path one. Although the pilot is of  $(2L + 2Q)$  samples, we only truncate out  $2L$  samples for estimation. Compared with (5), the received samples in the single-path case are

$$\mathbf{Y} = \beta \mathbf{a}(\theta) \mathbf{x}(\tau, \xi)^T + \mathbf{Z} \in \mathbb{C}^{M \times 2L}. \quad (26)$$

Since the pilot consists of two halves, we split  $\mathbf{Y}$  accordingly into  $\mathbf{Y} = [\mathbf{Y}_1 : \mathbf{Y}_2]$ , split  $\mathbf{x}(\tau, \xi)^T$  into  $\mathbf{x}(\tau, \xi)^T = [\mathbf{x}_1(\tau, \xi)^T : \mathbf{x}_2(\tau, \xi)^T]$ , and vectorize (26) into

$$\begin{bmatrix} \tilde{\mathbf{y}}_1 \\ \vdots \\ \tilde{\mathbf{y}}_2 \end{bmatrix} = \beta \begin{bmatrix} \mathbf{x}_1(\tau, \xi) \\ \vdots \\ \mathbf{x}_2(\tau, \xi) \end{bmatrix} \otimes \mathbf{a}(\theta) + \text{vec}(\mathbf{Z}), \quad (27)$$

where  $\tilde{\mathbf{y}}_i \triangleq \text{vec}(\mathbf{Y}_i)$ ,  $i = 1, 2$ .

In the single-path case, the JEVAR problem (14) reduces to a three-dimensional problem

$$\{\hat{\tau}, \hat{\xi}, \hat{\theta}\} = \arg \max_{\tau, \xi, \theta} \frac{\left| \begin{bmatrix} \tilde{\mathbf{y}}_1 \\ \tilde{\mathbf{y}}_2 \end{bmatrix}^H \left\{ \begin{bmatrix} \mathbf{x}_1(\tau, \xi) \\ \mathbf{x}_2(\tau, \xi) \end{bmatrix} \otimes \mathbf{a}(\theta) \right\} \right|^2}{\left\| \begin{bmatrix} \mathbf{x}_1(\tau, \xi) \\ \mathbf{x}_2(\tau, \xi) \end{bmatrix} \otimes \mathbf{a}(\theta) \right\|^2}. \quad (28)$$

Since  $\mathbf{x}_1(\tau, \xi)$ ,  $\mathbf{x}_2(\tau, \xi)$ , and  $\mathbf{a}(\theta)$  all have unit-modulus elements, the denominator in (28) is a constant; thus, (28) can be simplified as

$$\begin{aligned} \{\hat{\tau}, \hat{\xi}, \hat{\theta}\} &= \arg \max_{\tau, \xi, \theta} \left| \begin{bmatrix} \tilde{\mathbf{y}}_1 \\ \tilde{\mathbf{y}}_2 \end{bmatrix}^H \left\{ \begin{bmatrix} \mathbf{x}_1(\tau, \xi) \\ \mathbf{x}_2(\tau, \xi) \end{bmatrix} \otimes \mathbf{a}(\theta) \right\} \right|^2 \\ &= \arg \max_{\tau, \xi, \theta} \left| \mathbf{a}(\theta)^H \mathbf{Y}_1 \mathbf{x}_1(\tau, \xi)^* + \mathbf{a}(\theta)^H \mathbf{Y}_2 \mathbf{x}_2(\tau, \xi)^* \right|^2. \end{aligned} \quad (29)$$

Note that

$$\begin{aligned}\mathbf{x}_1(\tau, \xi) &= \mathbf{x}(\tau) \odot \mathbf{d}(\xi) \\ &= e^{j\frac{\pi\tau^2}{L}} \mathbf{s} \odot \mathbf{d}\left(\xi - \frac{\tau}{L}\right).\end{aligned}\quad (30)$$

Similarly,

$$\mathbf{x}_2(\tau, \xi) = e^{-j\frac{\pi\tau^2}{L}} \mathbf{s}^* \odot \mathbf{d}\left(\xi + \frac{\tau}{L}\right) e^{j2\pi\xi(Q+L)}.\quad (31)$$

where the term  $e^{j2\pi\xi(Q+L)}$  is the phase change over the duration of the first ZC sequence plus the suffix, and the prefix of the second ZC sequence due to the frequency offset.

Inserting (30) and (31) into (29) yields

$$\begin{aligned}\{\hat{\tau}, \hat{\xi}, \hat{\theta}\} &= \arg \max_{\tau, \xi, \theta} \left| \mathbf{a}(\theta)^H \mathbf{Y}_1 e^{-j\frac{\pi\tau^2}{L}} \text{diag}(\mathbf{s}^*) \mathbf{d}\left(-\xi + \frac{\tau}{L}\right) \right. \\ &\quad \left. + \mathbf{a}(\theta)^H \mathbf{Y}_2 e^{j\frac{\pi\tau^2}{L}} \text{diag}(\mathbf{s}) \mathbf{d}\left(-\xi - \frac{\tau}{L}\right) e^{-j2\pi\xi(Q+L)} \right|^2.\end{aligned}\quad (32)$$

Denoting

$$\tilde{\mathbf{Y}}_1 \triangleq \mathbf{Y}_1 \text{diag}(\mathbf{s}^*), \quad \tilde{\mathbf{Y}}_2 \triangleq \mathbf{Y}_2 \text{diag}(\mathbf{s}),\quad (33)$$

we simplify (32) as

$$\begin{aligned}\{\hat{\tau}, \hat{\xi}, \hat{\theta}\} &= \arg \max_{\tau, \xi, \theta} \left| e^{-j\frac{2\pi\tau^2}{L}} \mathbf{a}(\theta)^H \tilde{\mathbf{Y}}_1 \mathbf{d}\left(-\xi + \frac{\tau}{L}\right) \right. \\ &\quad \left. + e^{-j2\pi\xi(Q+L)} \mathbf{a}(\theta)^H \tilde{\mathbf{Y}}_2 \mathbf{d}\left(-\xi - \frac{\tau}{L}\right) \right|^2.\end{aligned}\quad (34)$$

The three-dimension optimization problem (34) can be solved using a standard Newton's iterative method, given a good initialization. In the next, we present an efficient method for the initialization estimation.

#### A. The JEVAR Estimation

Denoting

$$\zeta = \xi - \frac{\tau}{L}, \quad \eta = \xi + \frac{\tau}{L},\quad (35)$$

we transform (34) into

$$\begin{aligned}\{\hat{\zeta}, \hat{\eta}, \hat{\theta}\} &= \arg \max_{\zeta, \eta, \theta} \left| e^{-j\frac{\pi}{2}(\eta-\zeta)^2 L} \mathbf{a}(\theta)^H \tilde{\mathbf{Y}}_1 \mathbf{d}(-\zeta) \right. \\ &\quad \left. + e^{-j\pi(\eta+\zeta)(L+Q)} \mathbf{a}(\theta)^H \tilde{\mathbf{Y}}_2 \mathbf{d}(-\eta) \right|^2,\end{aligned}\quad (36)$$

where the two terms correspond to the two halves of the pilot.

If use only the first half pilot, we obtain a suboptimal estimation of  $\zeta$  and  $\theta$ :

$$\begin{aligned}\{\hat{\zeta}, \hat{\theta}\} &= \arg \max_{\zeta, \theta} \left| e^{-j\frac{\pi}{2}(\eta-\zeta)^2 L} \mathbf{a}(\theta)^H \tilde{\mathbf{Y}}_1 \mathbf{d}(-\zeta) \right|^2 \\ &= \arg \max_{\zeta, \theta} \left| \mathbf{a}(\theta)^H \tilde{\mathbf{Y}}_1 \mathbf{d}(-\zeta) \right|^2;\end{aligned}\quad (37)$$

similarly, if use only the second half pilot, we obtain a suboptimal estimation of  $\eta$  and  $\theta$ :

$$\begin{aligned}\{\hat{\eta}, \hat{\theta}\} &= \arg \max_{\eta, \theta} \left| e^{-j\pi(\eta+\zeta)(L+Q)} \mathbf{a}(\theta)^H \tilde{\mathbf{Y}}_2 \mathbf{d}(-\eta) \right|^2 \\ &= \arg \max_{\eta, \theta} \left| \mathbf{a}(\theta)^H \tilde{\mathbf{Y}}_2 \mathbf{d}(-\eta) \right|^2.\end{aligned}\quad (38)$$

We can estimate  $\zeta$  and  $\theta$ , denoted as  $\hat{\theta}_1$ , by applying a two-dimensional FFT (2D-FFT) to  $\tilde{\mathbf{Y}}_1$  and localizing the largest entry; similarly, we can estimate  $\eta$  and  $\theta$ , denoted as  $\hat{\theta}_2$ , by applying a 2D-FFT to  $\tilde{\mathbf{Y}}_2$ . Thus, the initial estimates are

$$\hat{\tau} = \frac{(\hat{\eta} - \hat{\zeta})\tilde{L}}{2}, \quad \hat{\xi} = \frac{\hat{\eta} + \hat{\zeta}}{2}, \quad \hat{\theta} = \frac{\hat{\theta}_1 + \hat{\theta}_2}{2}.\quad (39)$$

Given the initial estimation (39), we apply Newton's iterative method [8] to (34) for refined estimation of  $\tau, \xi$  and  $\theta$ .

We denote  $\boldsymbol{\psi} \triangleq [\tau, \xi, \theta]^T$  and the objective function of (34) is  $\Lambda$ . After calculating the Hessian matrix  $\mathbf{H} \in \mathbb{R}^{3 \times 3}$  and the Jacobian vector  $\mathbf{g} \in \mathbb{R}^{3 \times 1}$  of  $\Lambda(\boldsymbol{\psi})$ , we can update the estimation as

$$\boldsymbol{\psi}^{(i+1)} = \boldsymbol{\psi}^{(i)} - s\mathbf{H}^{-1}\mathbf{g},\quad (40)$$

where  $s$  is the step size determined by the backtracking line search method [8].

Now we see the great benefit of adopting the conjugate ZC sequences: the original three-dimensional estimation problem (34) is reduced to the two-dimensional problems (37)(38), which can be solved by using two-dimensional FFT twice, followed by the simple formula (39).

#### B. Computational Complexity

By using the conjugate ZC pair, the solution to the original three-dimensional problem (34) can be initialized via  $N_\theta \times N_f$  2D-FFTs applied to solved (37) and (38) followed by the simple algebra in (39), where  $N_\theta$  is the number of grids in the angle domain and  $N_f$  is that in the frequency domain. Such FFTs incurs  $O(MN_f \log_2(N_f) + N_f N_\theta \log_2(N_\theta))$  flops.

In contrast, a state-of-the-art approach, e.g., the one in [4] uses an initialization of the JEVAR estimate requiring  $O(N_\tau M N_f \log_2 N_f)$  flops, where  $N_\tau$  is the number of search grid points in time domain, which can be large when the time delay range is large (e.g.,  $N_\tau = 200$  for a delay range of  $100T_s$  with time grid interval  $0.5T_s$ ). Compared  $O(MN_f \log_2(N_f) + N_f N_\theta \log_2(N_\theta))$  with  $O(N_\tau M N_f \log_2 N_f)$ , the proposed method can be at least one order of magnitude faster thanks to adopting the conjugate pair of ZCs as the pilot.

### V. THE JEVAR IN MULTIPATH CASE

This section proceeds to study the multipath case. The key idea is to use the AP method [6] to decompose the multipaths into multiple single paths, to which the method in the previous section can be applied multiple times.

Applying the same algebraic manipulation that leads from (26) to (27), we can obtain from (5) that

$$\begin{bmatrix} \tilde{\mathbf{y}}_1 \\ \vdots \\ \tilde{\mathbf{y}}_2 \end{bmatrix} = \sum_{u=1}^U \beta_u \begin{bmatrix} \mathbf{x}_1(\tau_u, \xi_u) \\ \vdots \\ \mathbf{x}_2(\tau_u, \xi_u) \end{bmatrix} \otimes \mathbf{a}(\theta_u) + \text{vec}(\mathbf{Z}).\quad (41)$$

where  $\mathbf{x}_1$  and  $\mathbf{x}_2$  are as defined in (30) and (31).

Denote

$$\tilde{\mathbf{y}} = \begin{bmatrix} \tilde{\mathbf{y}}_1 \\ \vdots \\ \tilde{\mathbf{y}}_2 \end{bmatrix} \in \mathbb{C}^{2LM \times 1},\quad (42)$$

$$\tilde{\mathbf{x}}_u \triangleq \begin{bmatrix} \mathbf{x}_1(\tau_u, \xi_u) \\ \dots \\ \mathbf{x}_2(\tau_u, \xi_u) \end{bmatrix} \otimes \mathbf{a}(\theta_u) \in \mathbb{C}^{2LM \times 1}, \quad (43)$$

$$\tilde{\mathbf{X}} = [\tilde{\mathbf{x}}_1, \dots, \tilde{\mathbf{x}}_u, \dots, \tilde{\mathbf{x}}_U] \in \mathbb{C}^{2LM \times U}, \quad (44)$$

and  $\tilde{\mathbf{X}}_u \in \mathbb{C}^{2LM \times (U-1)}$  is obtained by striking  $\tilde{\mathbf{x}}_u$  from  $\tilde{\mathbf{X}}$ . By utilizing the properties of projection matrix, we have

$$\mathcal{P}(\tilde{\mathbf{X}}) = \mathcal{P}(\tilde{\mathbf{X}}_u) + \mathcal{P}\left\{\mathcal{P}^\perp(\tilde{\mathbf{X}}_u)\tilde{\mathbf{x}}_u\right\}, \quad (45)$$

where  $\mathcal{P}^\perp(\tilde{\mathbf{X}}_u) = \mathbf{I} - \mathcal{P}(\tilde{\mathbf{X}}_u)$ . Inserting (45) into the objective function of (14), we obtain

$$\{\hat{\tau}, \hat{\xi}, \hat{\theta}\} = \arg \max_{\tau, \xi, \theta} \tilde{\mathbf{y}}^H \left[ \mathcal{P}(\tilde{\mathbf{X}}_u) + \mathcal{P}\left\{\mathcal{P}^\perp(\tilde{\mathbf{X}}_u)\tilde{\mathbf{x}}_u\right\} \right] \tilde{\mathbf{y}}. \quad (46)$$

Given that  $\tilde{\mathbf{X}}_u$  is known and fixed (i.e.,  $\{\tau_k, \xi_k, \theta_k\}_{k=1, k \neq u}^U$  are known), (46) can be simplified as

$$\begin{aligned} \{\hat{\tau}_u, \hat{\xi}_u, \hat{\theta}_u\} &= \arg \max_{\tau_u, \xi_u, \theta_u} \tilde{\mathbf{y}}^H \mathcal{P}\left\{\mathcal{P}^\perp(\tilde{\mathbf{X}}_u)\tilde{\mathbf{x}}_u\right\} \tilde{\mathbf{y}} \\ &= \arg \max_{\tau_u, \xi_u, \theta_u} \frac{\left| \tilde{\mathbf{y}}^H \mathcal{P}^\perp(\tilde{\mathbf{X}}_u)\tilde{\mathbf{x}}_u \right|^2}{\tilde{\mathbf{x}}_u^H \mathcal{P}^\perp(\tilde{\mathbf{X}}_u)\tilde{\mathbf{x}}_u}; \end{aligned} \quad (47)$$

thus, the AP decomposes the multipath problem into multiple single paths.

We approximate the initial estimate of the  $u^{\text{th}}$  path as

$$\begin{aligned} \{\hat{\tau}_u, \hat{\xi}_u, \hat{\theta}_u\} &\approx \arg \max_{\tau_u, \xi_u, \theta_u} \frac{\left| \tilde{\mathbf{y}}^H \mathcal{P}^\perp(\tilde{\mathbf{X}}_u)\tilde{\mathbf{x}}_u \right|^2}{\tilde{\mathbf{x}}_u^H \tilde{\mathbf{x}}_u} \\ &= \arg \max_{\tau_u, \xi_u, \theta_u} \left| \tilde{\mathbf{y}}^H \mathcal{P}^\perp(\tilde{\mathbf{X}}_u)\tilde{\mathbf{x}}_u \right|^2, \end{aligned} \quad (48)$$

which can be solved the same way as presented in Section IV, before applying Newton's method to (47) for the refined estimation.

In the scenario where two paths have similar gains, it is likely that the parameters obtained from the two half pilots [cf. (37) and (38)] correspond to different reflections. To make sure the estimates from the two half ZCs are associated with the same path, after solving (37) and obtaining  $\hat{\theta}_u$ , we estimate  $\eta$  as

$$\hat{\eta}_u = \arg \max_{\eta_u} \left| \mathbf{a}(\hat{\theta}_u)^H \tilde{\mathbf{Y}}_2 \mathbf{d}(-\eta_u) \right|^2, \quad (49)$$

which is the same as (38) except for setting  $\theta$  to be  $\hat{\theta}_u$ .

To initialize the AP procedure, we assume the received signal contains only one path and estimate  $\{\hat{\tau}_1, \hat{\xi}_1, \hat{\theta}_1\}^{(1)}$  via

$$\{\hat{\tau}_1, \hat{\xi}_1, \hat{\theta}_1\}^{(1)} = \arg \max_{\tau_1, \xi_1, \theta_1} \left| \tilde{\mathbf{y}}^H \tilde{\mathbf{x}}_1 \right|^2, \quad (50)$$

where the superscript denotes the iteration index; thus  $\tilde{\mathbf{x}}_1^{(1)} = \mathbf{x}(\tau_1, \xi_1) \otimes \mathbf{a}(\theta_1)$  is obtained. Then we set  $\tilde{\mathbf{X}}_2 = \tilde{\mathbf{x}}_1^{(1)}$  and estimate  $\{\hat{\tau}_2, \hat{\xi}_2, \hat{\theta}_2\}^{(1)}$  from (48). Next we set  $\tilde{\mathbf{X}}_3 = [\tilde{\mathbf{x}}_1^{(1)}, \tilde{\mathbf{x}}_2^{(1)}]$  and estimate  $\{\hat{\tau}_3, \hat{\xi}_3, \hat{\theta}_3\}^{(1)}$ . This procedure continues until  $\{\hat{\tau}_U, \hat{\xi}_U, \hat{\theta}_U\}^{(1)}$  with  $\tilde{\mathbf{X}}_U = [\tilde{\mathbf{x}}_1^{(1)}, \tilde{\mathbf{x}}_2^{(1)}, \dots, \tilde{\mathbf{x}}_{U-1}^{(1)}]$ .

In the second round of iteration, first estimate  $\{\hat{\tau}_1, \hat{\xi}_1, \hat{\theta}_1\}^{(2)}$  according to (47) with  $\tilde{\mathbf{X}}_1 = [\tilde{\mathbf{x}}_2^{(1)}, \tilde{\mathbf{x}}_3^{(1)}, \dots, \tilde{\mathbf{x}}_U^{(1)}]$ . Then estimate  $\{\hat{\tau}_2, \hat{\xi}_2, \hat{\theta}_2\}^{(2)}$  according to (47) with  $\tilde{\mathbf{X}}_2 = [\tilde{\mathbf{x}}_1^{(2)}, \tilde{\mathbf{x}}_3^{(1)}, \dots, \tilde{\mathbf{x}}_U^{(1)}]$ ,

and so on. Proceed the iterations to update the parameters of each path until convergence. In the above derivations we assume that the number of multipaths  $U$  is known. In practice, it can be estimated using, e.g., the Akaike's information criterion [9].

## VI. SIMULATION RESULTS

This section evaluates the performance of the proposed scheme through numerical simulations. Consider a 6-antenna ULA with half wavelength inter-element spacing. The transmitted pilot is the concatenation of a pair of conjugate ZC sequences of length  $L = 250$  and  $\tilde{L} = 400$ , each with a length-15 prefix and a length-15 suffix, i.e.,  $Q = 30$ . The pulse shaper is a raised cosine filter with the roll-off factor  $\alpha = 0.3$ . The carrier frequency  $f_c = 2.4\text{GHz}$  and the bandwidth  $B = 20\text{MHz}$ , that is, the Nyquist sampling interval is  $T_s = 50\text{ns}$ . Each simulation result is based on 1000 Monte-Carlo trials.

The single-path LOS scenario settings are  $\theta = 5^\circ$ ,  $\xi = 3 \times 10^{-5}/T_s$  (or 600Hz),  $\tau = 1.2T_s$ , and  $\beta = e^{j\phi}$  with  $\phi$  being random. The propagation distance and velocity is  $\rho = 18\text{m}$  and  $v = 75\text{m/s}$ . Fig. 3 shows the RMSE estimation of the velocity, angle and range versus SNR. We can see that the RMSE results of the proposed scheme almost overlap with the CRBs (the derivations are given in the journal version of this paper). At the SNR 20dB, the RMSE of the range estimation is about 2cm, which is a striking result given only 20MHz bandwidth; the velocity estimation error is about 3m/s, and the angle estimation error is only  $0.01^\circ$ . Here we have used the range-delay translation  $\rho = \tau \times c$ , where  $c$  is the light speed, and the velocity-Doppler frequency offset translation  $v = \frac{c\xi}{f_c}$ .

Then we consider a two-path case where  $\xi = [3 \times 10^{-5}, 7 \times 10^{-5}]/T_s$ ,  $\theta = [5^\circ, 20^\circ]$ ,  $\tau = [1.2, 1.3]T_s$ , and  $\beta = [e^{j\phi_1}, 0.5e^{j\phi_2}]$  with  $\phi_1$  and  $\phi_2$  being random. The propagation distance and velocity of the two-path are  $\rho = [18, 19.5]\text{m}$  and  $v = [75, 175]\text{m/s}$ , respectively. Fig. 4 shows the RMSE estimation of the velocities, angles and ranges of the two paths, compared with their respective CRBs. The result verify the JEVAR's super-resolution capability to separate two closely spaced multipaths.

The third example simulates a harsh environment where two equal-power paths have  $\xi = [10^{-5}, 10^{-4}]/T_s$ ,  $\theta = [10^\circ, 15^\circ]$ , and  $\tau = [1.1, 1.1 + \Delta\tau]T_s$ . The SNR is 20dB. Fig. 5 compares the RMSE of the frequency offset, angle, and time delay estimates of the first path with varying time delay gap  $\Delta\tau$  between the paths. We simulate the SAGE method with the maximum iterations  $\kappa = 50, 200$  and 1000, while  $\kappa$  is 30 for the AP method. Fig. 5 indicates that the AP can achieve the CRB and outperforms the SAGE in this multipath environment, although the performance of the SAGE can be improved by running (many) more iterations. Take  $\Delta\tau = 0.25T_s$  for example, by using the SAGE ( $\kappa = 200$ ), the RMSEs of the frequency offset, angle and time delay estimation are about  $2 \times 10^{-5}/T_s$  (corresponding to 50m/s velocity error),  $1.1^\circ$  and  $0.06T_s$  (corresponding to 90cm ranging error); in contrast, the AP ( $\kappa = 30$ ) yields the RMSEs of the frequency offset, angle and time delay are about  $2.8 \times 10^{-6}/T_s$  (corresponding to

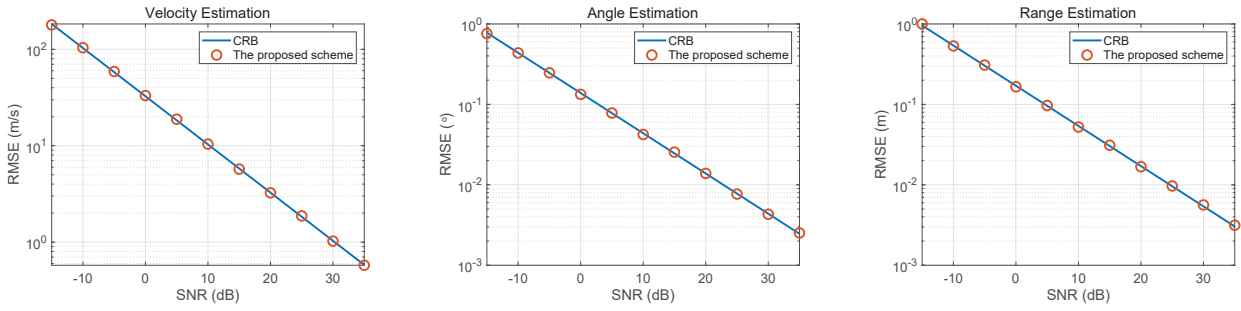


Fig. 3: The RMSEs of the velocity, angle and range estimation in the single-path case compared with the CRBs.

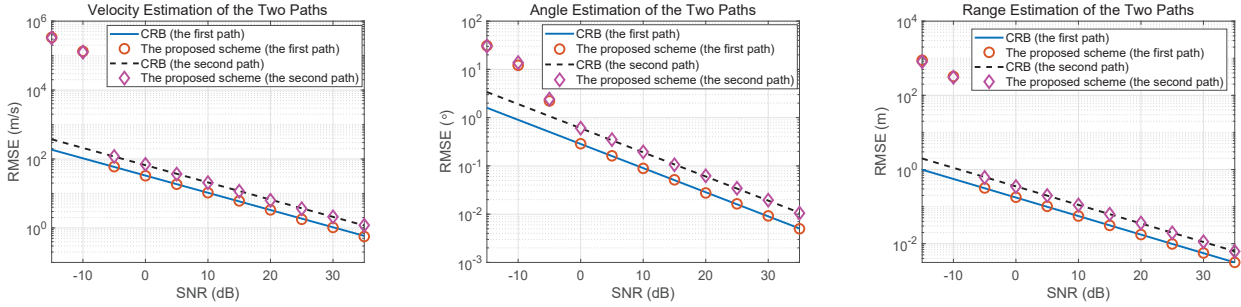


Fig. 4: The RMSEs of the velocity, angle and range estimation in the two-path case compared with the CRBs.

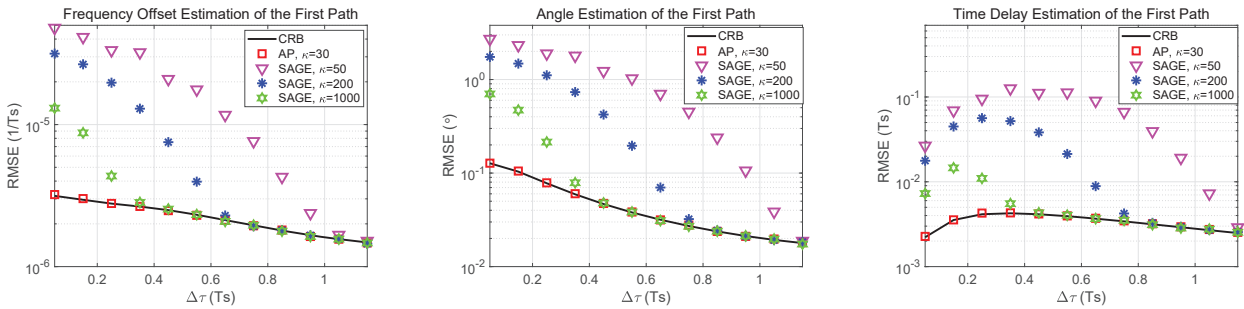


Fig. 5: Performance comparison between the AP with the SAGE in RMSEs of the LOS signal of the frequency offset, angle and time delay under different delay separation  $\Delta\tau$ ;  $\kappa$  is the maximum iterations constraint for the iterative algorithms.

7m/s velocity error),  $0.08^\circ$  and  $4 \times 10^{-3}T_s$  (corresponding to 6cm ranging error).

## VII. CONCLUSION

In this paper, we studied the joint estimation of the velocity, angle and range (JEVAR) of a target in a multipath environment, and introduced an efficient scheme – we have the target transmit a pair of conjugate ZC sequences and let the multi-antenna receiver conduct the maximum likelihood (ML) estimation. Using a waveform of 20MHz bandwidth, we can achieve the range estimation of centimeter-level precision, the AOA estimation of  $0.01^\circ$  precision, and the velocity estimation of one m/s precision, which makes the proposed scheme a promising technology for the localization and navigation related Internet of Things (IoT) applications.

## REFERENCES

- [1] L. Zhang and H. Wang, "Device-free tracking via joint velocity and AOA estimation with commodity WiFi," *IEEE Sensors Journal*, vol. 19, no. 22, pp. 10662–10673, 2019.
- [2] S. Kuutti, S. Fallah, K. Katsaros, M. Dianati, F. Mccullough, and A. Mouzakitis, "A survey of the state-of-the-art localization techniques and their potentials for autonomous vehicle applications," *IEEE Internet of Things Journal*, vol. 5, no. 2, pp. 829–846, 2018.
- [3] B. H. Fleury, M. Tschudin, R. Heddergott, D. Dahlhaus, and K. Ingeman Pedersen, "Channel parameter estimation in mobile radio environments using the SAGE algorithm," *IEEE Journal on Selected Areas in Communications*, vol. 17, no. 3, pp. 434–450, 1999.
- [4] F. Antreich, J. A. Nossek, and W. Utschick, "Maximum likelihood delay estimation in a navigation receiver for aeronautical applications," *Aerospace Science and Technology*, vol. 12, no. 3, pp. 256–267, 2008.
- [5] Y. Jiang, B. Daneshrad, and G. J. Pottie, "A practical approach to joint timing, frequency synchronization and channel estimation for concurrent transmissions in a MANET," *IEEE Transactions on Wireless Communications*, vol. 16, no. 6, pp. 3461–3475, 2017.
- [6] X. Wei, Y. Jiang, Q. Liu, and X. Wang, "Calibration of phase shifter network for hybrid beamforming in mmwave massive mimo systems," *IEEE Transactions on Signal Processing*, vol. 68, pp. 2302–2315, 2020.
- [7] D. Chu, "Polyphase codes with good periodic correlation properties (corresp.)," *IEEE Transactions on Information Theory*, vol. 18, no. 4, pp. 531–532, 1972.
- [8] S. Boyd and L. Vandenberghe, *Convex Optimization*. 2004.
- [9] H. Akaike, "Information theory and an extension of the maximum likelihood principle," *Springer New York*, 1998.